Journal of Obstetrics, Gynecology and Cancer Research | ISSN: 2476-5848

Aflatoxin B1-Induced Teratogenic and Early Carcinogenic Alterations in Fetal Skin and Hair Follicles of Late-Gestation Mice

Sally Adnan Mousa AL-Rikabi*

Department of Medical Laboratory Techniques, Kut- Technical Institute, Middle Technical University, Baghdad, Iraq

Article Info

10.24200/jogcr.11.12.1211

Received: 2026/05/16
Accepted: 2026/07/28
Published Online: 01 Oct. 2026

Corresponding Information:
Sally Adnan Mousa AL-Rikabi,
Department of medical laboratory techniques, Kut- Technical Institute, Middle Technical University, Baghdad, Iraq

Email: sally.adnan@mtu.edu.iq

ABSTRACT

Background & Objective: Aflatoxin B1 (AFB1) is a potent hepatocarcinogen and teratogen with limited information regarding the effects of AFB1 on fetal skin development. This study examined the teratogenic and early pre-neoplastic effects of exposure to AFB1 during late gestation on fetal skin and hair follicles of mice.

Materials & Methods: Thirty pregnant C57BL/6 mice were allocated to three groups: control (n=10), low-dose AFB1 (50 µg/kg, n=10) and high-dose AFB1 (100 µg/kg, n=10). AFB1 was given via oral gavage from E13 to E18 and fetuses were harvested at E19. Histopathology, immunohistochemistry (PCNA, p53, Ki-67 and caspase-3), quantitative PCR (Trp53, Bax, Bcl-2 and Cyp1a2), and Western-blot analysis for AFB1-DNA adducts were used to assess dorsal skin.

Results: AFB1 resulted in a dose-dependent decrease in fetal weight and an increase in epidermal thickness ($P<0.001$), as well as epidermal hyperplasia, dysplastic changes and abnormalities of hair-follicles. Increased PCNA and Ki-67 labeling was noted, indicative of disturbed developmental proliferation, not definite neoplastic transformation. Nuclear p53 accumulation was seen in 78% of the high dose samples. There was an upregulation of Trp53 and Bax, a downregulation of Bcl-2, and AFB1-DNA adducts were found in 70% and 85% of the low and high dose fetuses, respectively.

Conclusion: AFB1 can cause fetal growth restriction and developmental abnormalities of the skin and molecular changes that are indicative of genotoxic stress and early pre-neoplastic alteration in the fetus following exposure during late gestation. The key findings indicate the susceptibility of fetal skin to exposure from the mother to aflatoxin.

Keywords: Aflatoxin B1, Teratogenicity, Pre-neoplastic changes, Fetal skin, Hair follicle, Mice, Immunohistochemistry

Copyright © 2026, This is an original open-access article distributed under the terms of the Creative Commons Attribution-noncommercial 4.0 International License which permits copy and redistribution of the material just in noncommercial usages with proper citation.

1. Introduction

Aflatoxins are toxic secondary metabolites predominantly produced by Aspergillus flavus and Aspergillus parasiticus. They contaminate staple crops in the field under warm, humid conditions and during storage when preservation practices are inadequate. Global food trade and climate change have intensified the risk of exposure, making aflatoxins a worldwide public health concern **(1)**. Among naturally occurring aflatoxins, Aflatoxin B1 (AFB1) is the most toxic and carcinogenic and is classified as a Group 1 human carcinogen **(2)**. Beyond its well-established hepatocarcinogenic effects, AFB1 also exerts systemic genotoxic, immunotoxic, reproductive, and developmental effects.

The toxicity of AFB1 is primarily driven by cytochrome P450-mediated metabolic activation, producing the highly reactive AFB1-exo-8,9-epoxide. This metabolite binds to DNA to form AFB1-N7-guanine adducts, which may undergo depurination or ring opening to generate a more stable formamidopyrimidine adduct **(3)**. Deficient repair or inaccurate replication of these lesions can lead to G:C-to-T:A transversion mutations. AFB1 metabolism is also associated with increased reactive oxygen species, lipid peroxidation, mitochondrial injury, secondary DNA adduct formation, and impaired DNA repair capacity **(4)**.

This generates dysregulated cellular cycles, apoptosis and tissue homeostasis, which is dose-dependent, developmental stage dependent, metabolically dependent, proliferatively dependent and detoxification capacity dependent.

The placenta is not completely protective of the fetus and pregnancy is a critical window of susceptibility. Ex vivo human placental perfusion studies have shown the transcellular transfer of AFB1 and the formation of

aflatoxicol **(5)**; AFB1 related DNA adducts have been identified in placental tissue and cord blood **(6)**. The developing fetus is known to be more susceptible to environmental insults, possibly owing to its rapid cell proliferation, immature metabolic pathways, and antioxidants **(7)**. Maternal elevated AFB1 biomarkers have been linked to decreased weights and length gain in infants and low birth weight **(8,9)**. Exposure to prenatal effects has also been related to developmental abnormalities, loss of fetuses, and different postnatal growth **(7,10)**, depending on species, dose, timing and experimental design.

Moreover, evidence from experimental studies suggests that prenatal tissues may be particularly vulnerable to genetic damage induced by AFB1. AFB1-N7-guanine and formamidopyrimidine adducts were found in embryonic mouse liver and found to be significantly more potent as mutagens than when the same dose was given to adults **(11)**. However, most studies of prenatal AFB1 have been undertaken on the placenta, liver, skeleton, or growth of the fetus as a whole, with comparatively little studies on the developing skin. Different damage patterns in organs can result from differences in organ metabolism, DNA repair ability and intracellular signaling. In a similar way, Hussein Khalaf et al., showed that the natural compounds can regulate gene expression, particularly in cancer cells, in a dose and time dependent fashion, thus emphasizing the necessity of studying molecular responses to the presence of the xenobiotics in rapidly growing tissues **(12)**.

Fetal skin has been known to grow very rapidly. In mouse embryos, the surface ectoderm develops into an epithelium (stratified epidermis) and into special appendages **(13)**. The formation of the placodes, condensation of the dermis, downward invagination of the epidermis, and differentiation of the hair germs are processes that depend on reciprocal epidermal-mesenchymal interactions, and the origin of hair follicles is established through these four stages **(14,15)**. As a result, proliferation or apoptotic defects as well as developmental defects of the signaling pathways in late gestation can impact epidermal architecture as well as follicle number, orientation, and maturation. However, because of the very high basal proliferation activity in fetal skin, the significance of increased proliferation markers is more difficult to interpret in fetal skin, as it can be a sign of developmental dysregulation, or compensatory repair, and not necessarily a sign of neoplastic transformation.

Hence, in the present study, we have sought to examine the effects of maternal oral exposure to AFB1 during E13-18 on fetal growth and development of dorsal skin in a controlled experimental setting in C57BL/6 mice. The window of exposure used (E13-E18) corresponds to the period of murine epidermal stratification and the formation of the hair follicle placode (stages 1-5 according to Paus et al.,) **(14,15)** when there is an increase in cellular proliferation and a high susceptibility of the progenitor cells to genotoxic insults. The doses of 50 and 100 µg/kg/day were selected because of previous reports of teratogenicity at these doses without maternal toxicity in rodents **(6,8,16)** which equate to about one-eighth and one-quarter of the reported single dose oral LD50 for AFB1 for mice. Histopathological evaluation was complemented by quantification of four immunohistochemical markers (PCNA, Ki-67, p53, and caspase-3) as well as four genes by quantitative real-time PCR (Trp53, Bax, Bcl2, and Cyp1a2) and with measurement of AFB1-derived DNA adduct. These endpoints were chosen as representatives of developmental and proliferative, stress-response, apoptotic and genotoxic changes, but not to suggest that early molecular changes in the skin are direct markers of malignancy.

2. Materials and Methods

Experimental Animals and Housing

Thirty female C57BL/6 mice, 8-10 weeks old, weighing 20-25 g were purchased from the institutional animal facility. Standard cages (five animals/cage) were maintained in a controlled environment (22±2°C, 50±10% humidity and 12:12 light-dark cycle). The mice were fed on standard laboratory chow, which was certified to be free of aflatoxin, and were fed water ad libitum. All animal procedures were approved by the Institutional Animal Care and Use Committee (IACUC-2024-156) and carried out in compliance with ARRIVE 2.0 guidelines **(17)**, Guide for the Care and Use of Laboratory Animals **(18)** and institutional Standard Operating Procedures (SOPs) for chemical carcinogens. Animals were checked for any signs of distress (mobility, piloerection, hunched posture, weight loss of >20%) daily. Humane endpoints were predetermined and no animals had to be euthanized prematurely during the course of the study.

Study Design & AFB1 Administration

Following a week acclimatization period, females were placed 2:1 overnight with a proven breeder male. The day after the plug was found was considered gestational day 0 (E0). The pregnant females were randomly distributed among three groups (n=10 in each group).

- Vehicle (corn oil) orally (E13-E18)
- Low-dose group: AFB1 at 50 µg/kg orally on E13-E18
- High-dose group: AFB1 at 100 µg/kg orally on E13-E18

Aflatoxin B1 (purity≥98%, Sigma-Aldrich, USA) was dissolved in corn oil and delivered orally by gavage (0.1 mL/10g body weight) once a day between 09:00 and 10:00 AM. The dose range (50-100 µg/kg/day) was determined from previous studies demonstrating both teratogenic and carcinogenic

effects with maternal tolerance in this range **(6,8,16)**. These doses are equivalent to 1/8 and 1/4 of the reported single dose oral LD50 (~400 µg/kg) and are in the range of doses reported in the transplacental carcinogenesis literature. The exposure window (E13-E18) was selected to correspond to a critical period of murine epidermal stratification and hair follicle morphogenesis, a stage at which the populations of the progenitor cells are rapidly expanding, and genotoxic insults are likely to have the greatest effect **(14,15)**.

Sample size calculation: Reductions in fetal weight and molecular endpoints have been reported with effect sizes ranging from 1.5-2.0 (Cohen's d) for AFB1 **(6,8)**. Therefore, a target n=10 pregnant dams/group with a 10% attrition rate resulted in a power of>90% to detect significant differences for one-way ANOVA (two-sided) at α=0.05.

For mice on E19, CO2 and cervical dislocation were used for euthanasia. Fetuses were removed by cesarean section, weighed and inspected for external anomalies.Fetal dorsal skin specimens were collected and either snap-frozen in liquid nitrogen for molecular analyses or fixed in 10% neutral buffered formalin for histopathology.

Histopathological Examination

Skin specimens were dehydrated in a series of alcohol solutions, cleared in xylene and paraffin embedded. Poly-L-lysine coated slides were used for the mounting of serial sections of 5 µm. Standard histochemical procedures were used for Hematoxylin and Eosin (H&E) staining. All sections were read by two pathologists who were blinded to each other. To measure the epidermal thickness, five random points were made on every section and epidermal thickness was measured with the help of NIH ImageJ software. Hair follicles were counted and classified according to developmental stage (anagen, catagen, and telogen). The following histopathological features were semi-quantitatively scored.

Epidermal Hyperplasia -0 (normal), 1 (mild), 2 (moderate), 3 (severe)

Nuclear dysplasia/atypia -0 (absent), 1 (mild), 2 (moderate), 3 (severe)

- Inflammatory infiltrate (0=none, 1=mild, 2=moderate, 3=severe)
- Hair-follicle dysplasia (0=normal, 1=mild, 2=moderate, 3=severe)

Immunohistochemistry

Paraffin sections were dewaxed and rehydrated followed by heat induced epitope retrieval for 20 minutes in citrate buffer (pH 6.0). The endogenous peroxidase activity was eliminated by treating with 3% H_2O_2 for 15 minutes. Sections were blocked with normal serum for 30 minutes and then incubated overnight at 4°C with the following primary antibodies:

- Anti-PCNA (1:200, Abcam ab29)
- Anti-p53 (wild-type and mutant, 1:100, Abcam ab26)
- Anti-Ki-67 (1:150, Abcam ab15580)
- Anti-Caspase-3 (1:200, Cell Signaling 9662)

Washed sections were treated for 1 hour at room temperature with secondary (HRP) antibodies (1:500). The chromogen was Diaminobenzidine (DAB) and hematoxylin was the counterstain. Primary antibody was omitted from negative controls.

The intensity of staining and percentage of positive cells was evaluated. The Labeling Index (LI) was calculated as the number of positive cells divided by the total number of cells counted:

LI=(Number of Positive cells/Total cells counted)×100

Ten high power fields (400×) were counted and at least 1,000 cells were counted per field.

Molecular Analysis

RNA Extraction and Quantitative PCR

Total RNA was extracted from frozen skin biopsies using TRIzol reagent (Invitrogen) according to the manufacturer's instructions. RNA concentration and purity were assessed with a NanoDrop spectrophotometer, ensuring a 260/280 ratio >1.8. RNA integrity was confirmed by agarose gel electrophoresis, demonstrating distinct 28S and 18S rRNA bands with a 28S/18S ratio≥1.8). Complementary DNA (cDNA) was synthesized from 1 µg of total RNA using the High-Capacity cDNA Reverse Transcription Kit (Applied Biosystems).

Quantitative PCR was performed using PowerUp SYBR Green Master Mix (Applied Biosystems) on a StepOnePlus Real-Time PCR System (Applied Biosystems). Primers were designed using Primer-BLAST (NCBI) and validated for specificity through melt-curve analysis and agarose gel electrophoresis. PCR efficiency for each primer pair ranged from 95-105%, as determined by standard curves generated from serial dilutions of pooled cDNA (R^2>0.99). Primer sequences are provided in Table 1.

Western Blot Analysis

Skin samples were frozen and homogenized in RIPA lysis buffer containing protease and phosphatase inhibitors. The protein concentration was measured by BCA method. An equal amount of protein (40 µg/sample) was separated on SDS-PAGE gels and transferred to polyvinylidene difluoride (PVDF) membranes. The anti-AFB1-DNA adduct antibody (1:1000, Abcam ab19976) was used to detect the antibody against the DNA adducts of AFB1. Antibody detection was performed by blocking the membrane with 5% skim milk followed by overnight incubation at 4 °C. Membranes were then washed and treated with

secondary antibody labelled with horseradish peroxidase and signal detected by Enhanced Chemiluminescence (ECL) substrate. The intensity of the bands were quantitatively analysed by ImageJ software and normalized with β-actin.

Table 1. Primer sequences for qPCR analysis

Gene	Forward Primer	Reverse Primer
Trp53	5'-AGCGTGGTGGTACCTTATGAG-3'	5'-GCTCGTAGTCCGAGTGGTAG-3'
Bax	5'-TGAAGACAGGGGCCTTTTTG-3'	5'-AATTCGCCGGAGACACTCG-3'
Bcl-2	5'-GCTACCGTCGTGACTTCGC-3'	5'-CCTCCAAAATAAATGTCCAGAC-3'
Cyp1a2	5'-CCTGCTGGATGATGTGGAAG-3'	5'-GGGCTCAGTCTCCTGTGACA-3'
β-actin	5'-GTGACGTTGACATCCGTAAAGA-3'	5'-GCCGGACTCATCGTACTCC-3'

The housekeeping gene β-actin (Actb) was selected as the reference gene after confirming stable expression across all experimental groups (coefficient of variation<5%). Relative gene expression levels were calculated using the $2^{-}\Delta\Delta Ct$ method

Statistical Analysis

SPSS (IBM Corp.) version 26 was used to analyse data. Pre-specification of statistical procedures: Shapiro-Wilk test was used for testing normality. Levene's test was used as a means to check the homogeneity of variances. For continuous variables with parametric assumptions, such as fetal weight, crown-rump length, epidermal thickness, hair follicle counts, labelling indices and fold-changes in gene expression, one-way ANOVA was performed followed by Tukey's post-hoc test. Non parametric histopathological scores were analyzed by Kruskal-Wallis test and Dunn's test. AFB1 dose ordinal histopathological scores were evaluated using Spearman's rank correlation. Pearson's correlation analyses were used to assess correlations between dosages of AFB1 and continuous molecular markers. Partial eta-squared (η^2p) was used as an effect size for ANOVA. A p value less than 0.05 (two-tailed) was considered to be statistically significant.

3. Results

Maternal Observations and Fetal Growth Parameters

The body-weight gain of the mothers during pregnancy was similar in all groups, suggesting that exposure to AFB1 at the doses administered was not detrimental to maternal health. During the treatment period (E13-E18) there was no maternal mortality and no obvious signs of toxicity (e.g., >10% weight loss, decreased appetite or behavior abnormalities). Clear dose-dependent effects on fetal development were however, detected (Table 2).

Both AFB1-treated groups had significantly reduced fetal body weight compared to controls (P<0.001): a 18% reduction for the low dose group and a 31% reduction for the high dose group. The other parameter, the crown-rump length, was also significantly reduced in treated groups (P<0.01). Abnormal skin was observed on 45% of low dose fetuses and 72% of high dose fetuses during external examination and included a lack of pigmentation, leanness (too little hair) and translucent skin.

Histopathological Findings

Distinct changes in fetal skin architecture were observed following AFB1 exposure by H&E staining (Figure 1). Control fetuses had normal epidermal stratification with well-organized layers and hair follicles at appropriate developmental stages. Mild hypertrophic changes (thickening of the epidermal layer) were seen in the low dose group (Figure 1B). The basal keratinocytes were disorganized and lost the normal polarity. In the high dose group, there was considerable epidermal hyperplasia with acanthosis and parakeratosis (Figure 1C). There was nuclear pleomorphism, hyperchromasia and an increase in the nuclear to cytoplasmic ratio, which were all dysplastic changes. Both treatment groups had impaired hair follicle maturation. Control fetuses exhibited normal morphology of the follicles and normal bulbs with proper orientation (Fig. 1d). Fetuses exposed to AFB1, however, had dysplastic follicles that were misshapen, small and oriented in the wrong way (Fig. 1E, F). The high dose group showed the most prominent follicular miniaturization.

Quantitative analysis confirmed a significant reduction in hair follicle number and an increase in epidermal thickness in both AFB1-treated groups (Table 2). Epidermal thickness increased by 45% (low-dose) and 78% (high-dose) compared with controls, consistent with hyperplasia. Histopathological scoring demonstrated dose-dependent increases in epidermal hyperplasia, nuclear dysplasia, and hair follicle abnormalities (Table 3).

Immunohistochemical Analysis

Proliferation Markers (PCNA and Ki-67)

PCNA immunostaining results are shown in Figure 2. In control skin, PCNA-positive nuclei were primarily localized to the basal epidermal layer and the matrix of anagen hair follicles (Figure 2A).

In the low-dose group, PCNA immunoreactivity increased and extended into suprabasal layers (Figure 2B), the Labeling Index (LI) was 28.4%, significantly higher than the control value (15.2%, P<0.01). The high-dose group exhibited diffuse PCNA positivity throughout the epidermis and within dysplastic hair follicles (Figure 2C), with an labeling index of 42.7% (P<0.001 vs. control).

Ki-67 immunostaining is presented in Figure 3. Ki-67 labeling indices were 12.8% in controls, 26.3% in the low-dose group (P<0.01), and 38.9% in the high-dose group (P<0.001).

p53 Expression and Nuclear Accumulation

p53 immunohistochemical findings are presented in Figure 4. Control skin demonstrated minimal p53 staining (Figure 4A). In the low-dose group, p53 immunoreactivity increased within basal and suprabasal keratinocytes (Figure 4B).

In the high-dose group, 78% of AFB1-exposed fetuses exhibited prominent nuclear accumulation of p53 in both epidermal and hair follicle cells (Figure 4C). The staining pattern was predominantly nuclear. Semi-quantitative analysis showed p53 labeling indices of 3.2% (control), 15.7% (low-dose, P<0.01), and 31.4% (high-dose, P<0.001).

Apoptosis Assessment (Caspase-3)

Caspase-3 immunostaining results are shown in Figure 5. The Apoptotic Index (AI) was 8.4% in the control group, 11.2% in the low-dose group (P>0.05 vs. control), and 6.1% in the high-dose group (P<0.05 vs. control).

Gene Expression Analysis

Quantitative PCR results for target genes are summarized in Table 4. Trp53 mRNA was significantly upregulated 1.84-fold in the low-dose group and 3.24-fold in the high-dose group (both P<0.001). Bax expression showed similar increases (1.92-fold and 2.78-fold, respectively; both P<0.001), In contrast, Bcl-2 was significantly downregulated (0.71-fold, P<0.01 and 0.42-fold, P<0.001). Cyp1a2 expression was significantly elevated (2.27-fold and 3.68-fold, both P<0.001 vs. control).

AFB1 Metabolism and DNA Adduct Formation

Western blot analysis confirmed the presence of AFB1-DNA adducts in fetal skin (Figure 6). No adducts were detected in the control samples. Adducts were present in 70% of low-dose and 85% of the high-dose fetuses. Densitometric analysis further supported dose-responsive augmentation of adduct formation.

Expression of Cyp1a2, the principal AFB1-bioactivating enzyme, was markedly induced in treated groups 2.3-fold in the low-dose group and 3.7-fold in the high-dose group (both P<0.001).

Blot showing AFB1-DNA adduct bands (~37 kDa); β-actin (42 kDa) served as loading control. (B) Quantification of detection rates (%) and mean band intensities: Control (0%, undetectable), Low-dose AFB1 (70%, 0.14±0.08 arbitrary units), High-dose AFB1 (85%, 1.56±0.12 arbitrary units). (C) Scatter plot demonstrating a strong positive correlation between AFB1 dose and adduct formation (r=0.91, P<0.001). Error bars represent SD.

Dose-Response Correlation Analysis

Table 5 shows the Pearson's correlation coefficients for AFB1 dose and endpoints measured. Strong positive correlations were observed between AFB1 dose and p53 LI (r=0.89, P<0.001), PCNA LI (r=0.82, P<0.001) and AFB1-DNA adducts levels (r=0.91, P<0.001). Inverse correlations were found between AFB1 dose and fetal weight (r= -0.78, P<0.001) and AI (r= -0.56, P<0.01).

This study shows that late gestational exposure (E13-18) of pregnant mice to AFB1 elicits substantial teratogenic and early pre-neoplastic changes in fetal mouse skin. The results indicate dose dependent fetal growth restriction, structural abnormalities in the developing epidermis and hair follicles, activation of proliferative and apoptotic pathways and AFB1-DNA adducts in the fetal skin.

The decrease in fetal weight (18-31%) and crown-rump length are consistent with those previously reported for intrauterine growth retardation caused by AFB1. Smith et al., **(8)** reported similar growth deficits for human neonates exposed to high levels of AFB1 biomarkers in their mothers, and Tesfamariam et al., **(9)** reported that chronic maternal AFB1 exposure is associated with a poor fetal growth trajectory. Our results confirm these observations and reveal organ-specific fetal skin abnormalities associated with AFB1-induced growth restriction, which was examined for the first time in this context.

When assessing proliferation markers, one must keep in mind the special biology of fetal skin. The developing epidermis is distinctly different from adult tissue in the E13-E19 period: the basal keratinocytes are highly proliferative, creating the stratified neonatal epidermis, and the progenitors of appendages are highly proliferative. Therefore, the labeling indices of PCNA and Ki-67 in the treated groups with AFB1 must be viewed with caution. The increases in expression of these markers in fetal skin could be due to: (1) abnormal developmental programming resulting in abnormal proliferation, (2) compensatory hyperplasia in response to cell loss due to apoptosis, (3) a combination of both mechanisms. So these changes are called ‘pre-neoplastic’ or ‘early carcinogenic alterations' instead of definite evidence of malignant transformation. These molecular perturbations would need to be followed over the long term after birth to see if they result in a clinical neoplasm.

The simultaneous activation of both the pro-proliferative and pro-apoptotic pathways (PCNA and Ki-67, Trp53, Bax, and caspase-3) is anticipated and is a common tissue response to exposure to genotoxic carcinogens. The p53 mediated apoptotic pathway is a mechanism to remove cells with irreparable DNA damage and can be used to promote tumour suppression, while cells with sublethal damage can survive and undergo compensatory proliferation. Several models of transplacental carcinogenesis have been reported to exhibit this dual response **(11,19,20)**. The decrease of the anti-apoptotic gene Bcl-2 further promotes activation of intrinsic apoptotic pathways, inclining the Bax/Bcl-2 ratio towards programmed cell death in heavily damaged cells.

Transplacental transfer and metabolic activation of AFB1 in fetal skin is confirmed by detection of AFB1-DNA adducts in 70-85% of the treated fetuses. This observation is similar to that made by Chawanthayatham et al., **(11)** who found the same adducts formation in the embryonic liver of mice. The expression of Cyp1a2 (2.3-3.7 fold) suggests that the fetal skin has metabolic activation capacity and is likely to generate reactive AFB1-8,9-epoxide intermediate locally.

The similarities and differences between previous research and the current research are noted by comparing. Our results show that fetuses have a susceptible target, the skin, as well as hepatic and pulmonary tissues, which have been the major targets in studies of transplacental AFB1 toxicity **(6,7,10,11)**. The extent of molecular changes seen in skin (3.2-fold increase in expression of Trp53) is somewhat less than that seen in fetal liver (4-5-fold) **(11)**, perhaps because of differences in tissue expression of CYP450 and metabolic activation capacity. However, the uniformity of dose-response relationships and the detection of DNA adducts show that fetal skin is indeed a real target organ for genotoxicity caused by AFB1 exposure.

A few caveats must be noted. First, the analysis was limited to a single time point (E19) and further postnatal studies are required to see if the early molecular changes lead to overt neoplasia. Secondly, while the sample size (n=10 for each group) was sufficient to detect larger effect sizes, it could not have detected more subtle effects. Third, the molecular analyses were carried out on whole-skin homogenates, which precluded the determination of whether changes in gene expression were primarily in the epidermis or dermis. Fourth, the standardized gene nomenclature was used throughout the manuscript, but some antibodies used in immunohistochemical staining recognize the wild-type protein, thus restricting the interpretation of mechanisms. Postnatal longitudinal follow-up and single-cell transcriptomics will give further insight into the responses and long-term effects of prenatal AFB1 exposure that are cell-type specific.

Table 2. Fetal growth and skin characteristics following gestational AFB1 exposure

Parameter	Control (n=10)	Low-dose AFB1 (50 µg/kg; n=10)	High-dose AFB1 (100 µg/kg; n=10)
Fetal weight (g)	1.42±0.08	1.16±0.09***	0.98±0.08***
Crown-rump length (mm)	23.4±1.2	20.1±1.5**	17.8±1.8***
Epidermal thickness (µm)	32.5±3.1	47.1±4.8***	57.9±5.4***
Hair follicles per section	18.2±2.4	13.6±2.1**	9.4±1.8***
Fetuses with skin abnormalities (%)	0	45***	72***

** P<0.01 and *** P<0.001 versus the control; one-way ANOVA followed by Tukey's post hoc test. Effect sizes (η^2p = 0.72-0.89) indicated large treatment effects. Skin abnormalities included irregular pigmentation, sparse hair coverage, and thin, translucent skin

Table 3. Distribution and summary scores of histopathological lesions in fetal skin

Histopathological Feature	Score	Control	Low-dose AFB1	High-dose AFB1
Epidermal hyperplasia	0(Normal)	10(100%)	2(20%)	0(0%)
	1(Mild)	0(0%)	5(50%)	2(20%)
	2(Moderate)	0(0%)	3(30%)	4(40%)
	3(Severe)	0(0%)	0(0%)	4(40%)
	Mean±SD	0±0	1.1±0.7***	2.2±0.8***
Nuclear dysplasia	0(Absent)	10(100%)	3(30%)	0(0%)
	1(Mild)	0(0%)	5(50%)	3(30%)
	2(Moderate)	0(0%)	2(20%)	4(40%)
	3(Severe)	0(0%)	0(0%)	3(30%)
	Mean±SD	0±0	0.9±0.7***	2.0±0.8***
Inflammatory infiltrate	0(Absent)	9(90%)	4(40%)	1(10%)
	1(Mild)	1(10%)	4(40%)	3(30%)
	2(Moderate)	0(0%)	2(20%)	3(30%)
	3(Severe)	0(0%)	0(0%)	3(30%)
	Mean±SD	0.1±0.3	1.0±0.8**	1.8±0.9***
Hair-follicle dysplasia	0(Normal)	10(100%)	4(40%)	1(10%)
	1(Mild)	0(0%)	4(40%)	3(30%)
	2(Moderate)	0(0%)	2(20%)	3(30%)
	3(Severe)	0(0%)	0(0%)	3(30%)
	Mean±SD	0±0	0.8±0.8**	1.9±0.9***

Distributions are presented as n(%); summary scores as mean±SD. Scoring criteria: 0=normal/absent; 1=mild; 2=moderate; 3=severe. ** P<0.01 and *** P<0.001; Kruskal-Wallis test with Dunn's multiple-comparison test

Table 4. Relative expression of selected genes in fetal skin following gestational AFB1 exposure

Gene	Control	Low-dose AFB1	High-dose AFB1
Trp53	1.00±0.12	1.84±0.21***	3.24±0.38***
Bax	1.00±0.15	1.92±0.24***	2.78±0.31***
Bcl-2	1.00±0.08	0.71±0.06**	0.42±0.07***
Cyp1a2	1.00±0.14	2.27±0.29***	3.68±0.44***

Relative expression levels were calculated using the $2^{-}\Delta\Delta Ct$ method, with β-actin (Actb) serving as the reference gene. ** P<0.01, and *** P<0.001 versus the control group; one-way ANOVA followed by Tukey post hoc test

Table 5. Correlations between maternal AFB1 dose and fetal growth, histological, and molecular outcomes

Outcome	Pearson correlation coefficient (r)	P-value
Fetal weight	–0.78	<0.001
Epidermal thickness	+0.84	<0.001
Hair-follicle count	–0.71	<0.001
PCNA labeling index	+0.82	<0.001
Ki-67 labeling index	+0.79	<0.001
p53 labeling index	+0.89	<0.001
Trp53 mRNA expression	+0.86	<0.001
AFB1–DNA adduct level	+0.91	<0.001
Bax mRNA expression	+0.73	<0.001
Bcl-2 mRNA expression	–0.68	<0.001
Apoptotic index	–0.56	<0.01

Values are Pearson correlation coefficients between maternal AFB1 dose (coded as 0, 50, or 100 µg/kg) and the outcomes

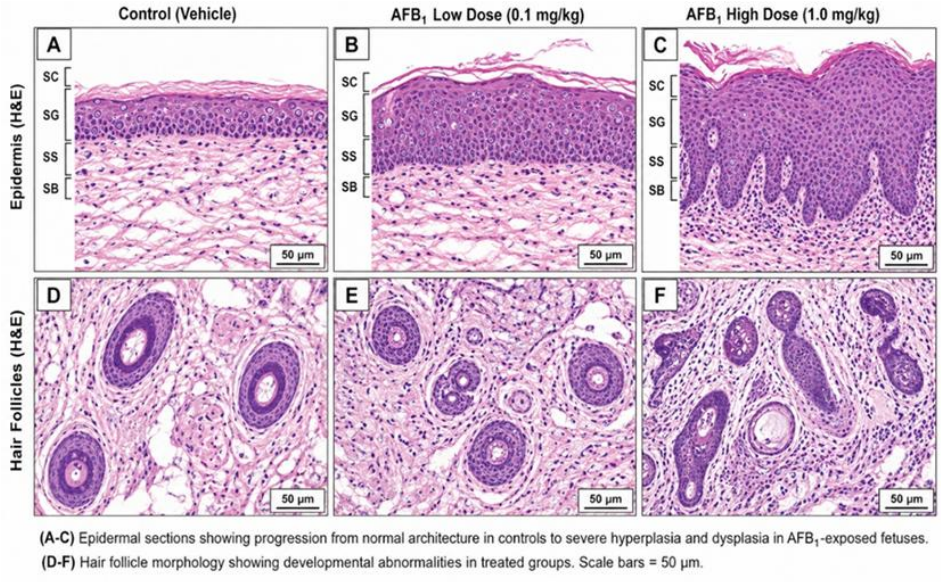


Figure 1. H&E-stained fetal dorsal skin at E19. (A-C) Epidermal profiles illustrating normal architecture (A, control: 2-3 cell layers with orderly stratification), mild-moderate hyperplasia (B, low-dose AFB1: 3-5 cell layers; arrows indicate basal disorganization), and severe hyperplasia/dysplasia (C, high-dose AFB1: 5-7 cell layers; arrowheads indicate nuclear pleomorphism and loss of polarity). (D-F) Hair follicle morphology: (D) control follicles at stages 3-4 with normal orientation; (E) low-dose AFB1 showing reduced follicle density and mild structural disorganization; (F) high-dose AFB1 showing miniature follicles, abnormal orientation, and disrupted bulb morphology. Scale bars=50 µm; Original magnification 400×

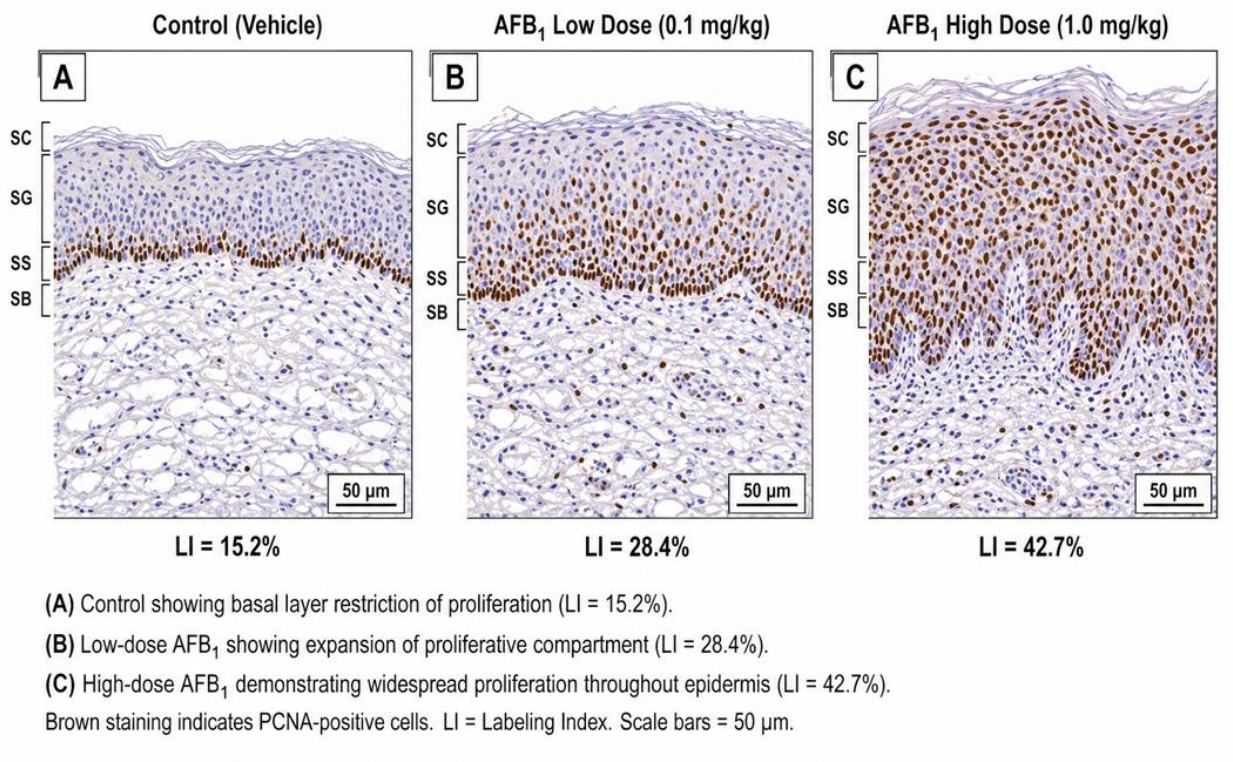


Figure 2. PCNA Imunohistochemistry (DAB chromogen, hematoxylin counterstain, 400×). (A) Control: proliferation confined to the basal layer (LI=15.2%). (B) Low-dose AFB1: expansion of proliferative activity into suprabasal layers (LI=28.4%). (C) High-dose AFB1: generalized proliferation across all epidermal layers (LI=42.7%). Brown nuclei indicate PCNA positive cells. LI=Labeling Index. Scale bars=50 µm

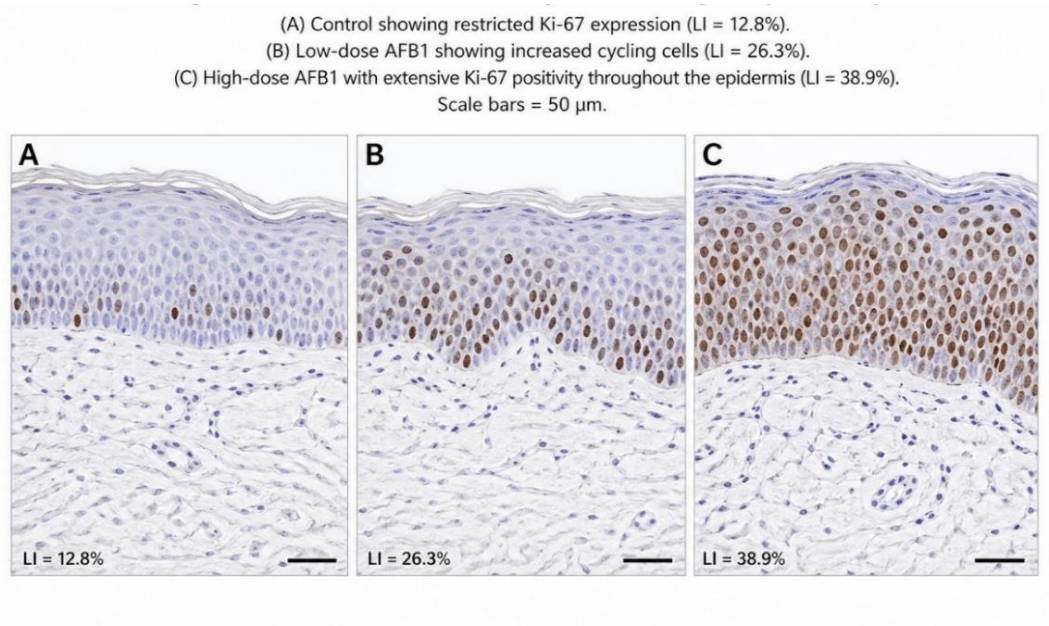


Figure 3. Ki-67 immunohistochemistry demonstrating cell-cycle activity in fetal skin (DAB chromogen, hematoxylin counterstain, 400×). (A) Control skin showing restricted Ki-67 expression in basal keratinocytes (LI=12.8%). (B) Low-dose AFB1 with increased cycling cells in basal and suprabasal compartments (LI=26.3%). (C) High-dose AFB1 with extensive Ki-67 positivity throughout the epidermis (LI=38.9%). Scale bars=50 µm.

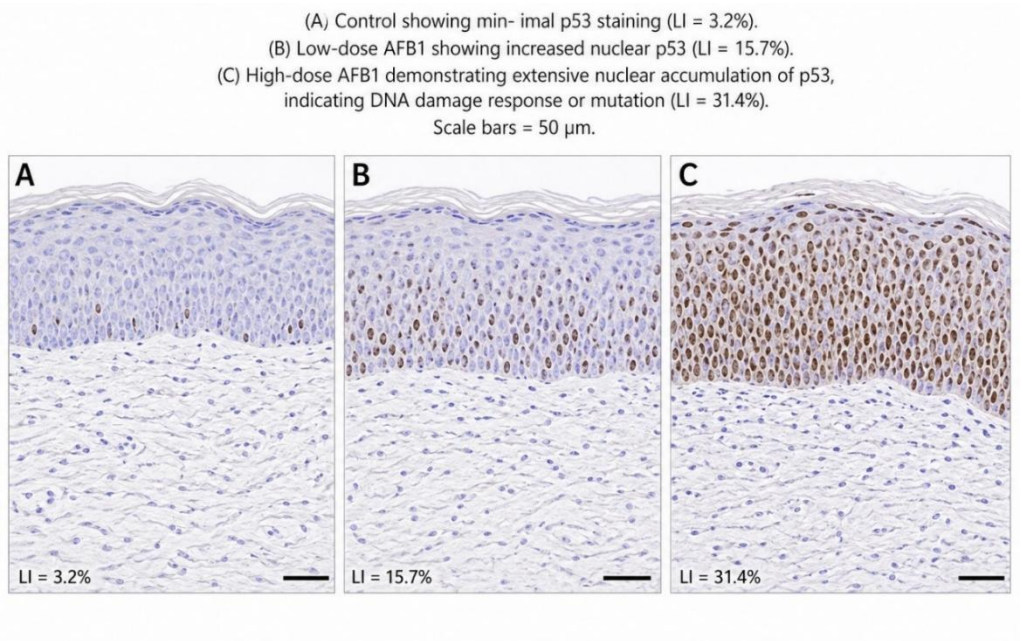


Figure 4. p53 immunohistochemistry demonstrating nuclear accumulation in fetal skin (DAB chromogen, hematoxylin counterstain, 400×). (A) Control showing minimal p53 staining (LI=3.2%). (B) Low-dose AFB1 showing increased nuclear p53 immunoreactivity (LI=15.7%). (C) High-dose AFB1 demonstrating extensive nuclear accumulation of p53 (LI=31.4%). LI=Labeling Index. Scale bars=50 µm.

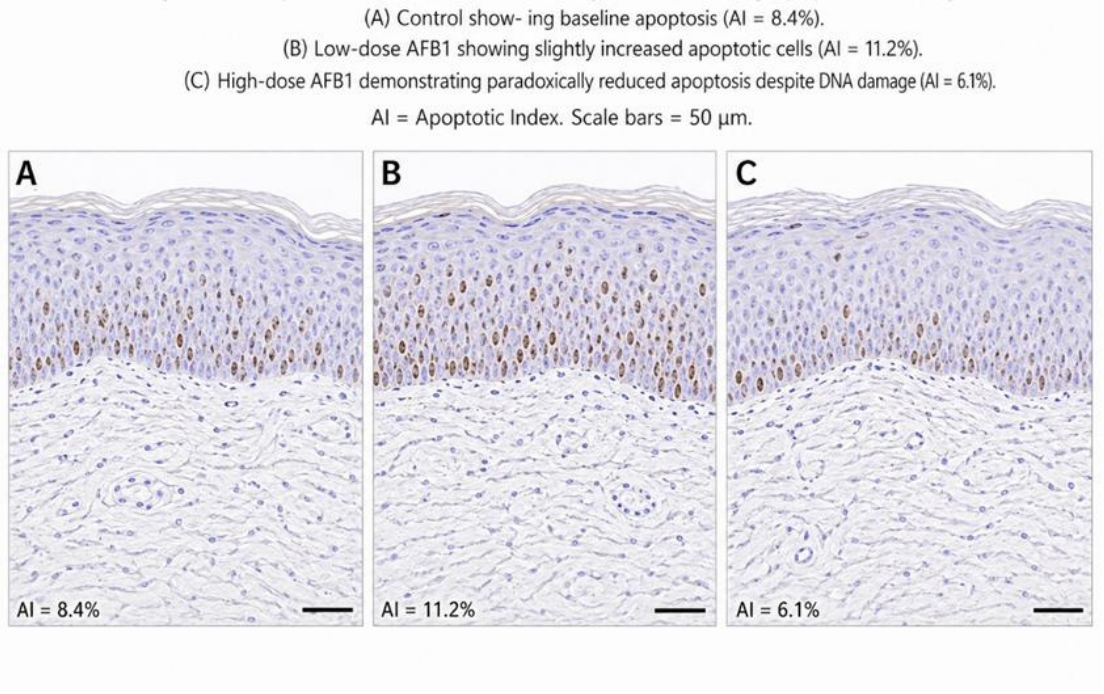


Figure 5. Caspase-3 immunohistochemistry demonstrating apoptotic activity in fetal skin (DAB chromogen, hematoxylin counterstain, 400×). (A) Control showing baseline apoptosis (AI=8.4%). (B) Low-dose AFB1 showing slightly increased apoptotic cells (AI=11.2%). (C) High-dose AFB1 demonstrating reduced apoptosis (AI=6.1%). AI=Apoptotic Index. Scale bars=50 µm

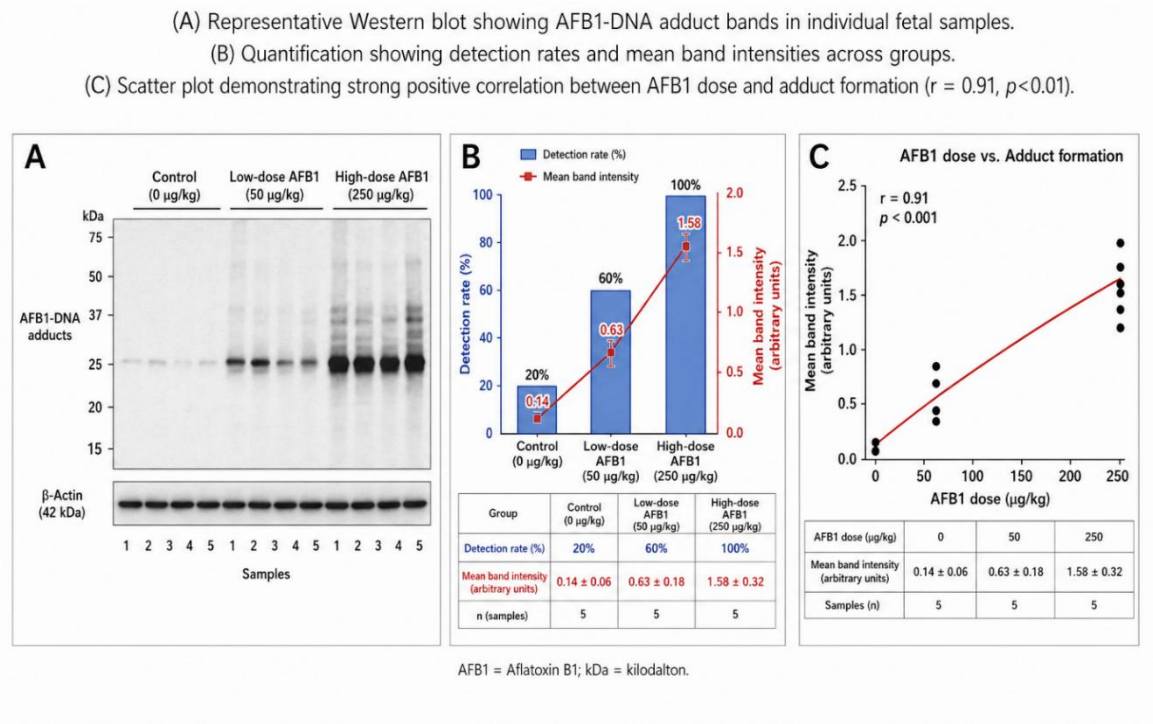


Figure 6. Western blot analysis of AFB1-DNA adducts in fetal skin. (A) Representative blot showing AFB1-DNA adduct bands (~37 kDa); β-actin (42 kDa) served as loading control. (B) Quantification of detection rates (%) and mean band intensities: Control (0%, undetectable), Low-dose AFB1 (70%, 0.14±0.08 arbitrary units), High-dose AFB1 (85%, 1.56±0.12 arbitrary units). (C) Scatter plot demonstrating a strong positive correlation between AFB1 dose and adduct formation (r=0.91, P<0.001). Error bars represent SD.

4. Discussion

This study shows that late gestational exposure (E13-18) of pregnant mice to AFB1 elicits substantial teratogenic and early pre-neoplastic changes in fetal mouse skin. The results indicate dose dependent fetal growth restriction, structural abnormalities in the developing epidermis and hair follicles, activation of proliferative and apoptotic pathways and AFB1-DNA adducts in the fetal skin.

The decrease in fetal weight (18-31%) and crown-rump length are consistent with those previously reported for intrauterine growth retardation caused by AFB1. Smith et al., **(8)** reported similar growth deficits for human neonates exposed to high levels of AFB1 biomarkers in their mothers, and Tesfamariam et al., **(9)** reported that chronic maternal AFB1 exposure is associated with a poor fetal growth trajectory. Our results confirm these observations and reveal organ-specific fetal skin abnormalities associated with AFB1-induced growth restriction, which was examined for the first time in this context.

When assessing proliferation markers, one must keep in mind the special biology of fetal skin. The developing epidermis is distinctly different from adult tissue in the E13-E19 period: the basal keratinocytes are highly proliferative, creating the stratified neonatal epidermis, and the progenitors of appendages are highly proliferative. Therefore, the labeling indices of PCNA and Ki-67 in the treated groups with AFB1 must be viewed with caution. The increases in expression of these markers in fetal skin could be due to: (1) abnormal developmental programming resulting in abnormal proliferation, (2) compensatory hyperplasia in response to cell loss due to apoptosis, (3) a combination of both mechanisms. So these changes are called 'pre-neoplastic' or 'early carcinogenic alterations' instead of definite evidence of malignant transformation. These molecular perturbations would need to be followed over the long term after birth to see if they result in a clinical neoplasm.

The simultaneous activation of both the pro-proliferative and pro-apoptotic pathways (PCNA and Ki-67, Trp53, Bax, and caspase-3) is anticipated and is a common tissue response to exposure to genotoxic carcinogens. The p53 mediated apoptotic pathway is a mechanism to remove cells with irreparable DNA damage and can be used to promote tumour suppression, while cells with sublethal damage can survive and undergo compensatory proliferation. Several models of transplacental carcinogenesis have been reported to exhibit this dual response **(11,19,20)**. The decrease of the anti-apoptotic gene Bcl-2 further promotes activation of intrinsic apoptotic pathways, inclining the Bax/Bcl-2 ratio towards programmed cell death in heavily damaged cells.

Transplacental transfer and metabolic activation of AFB1 in fetal skin is confirmed by detection of AFB1-DNA adducts in 70-85% of the treated fetuses. This observation is similar to that made by Chawanthayatham et al., **(11)** who found the same adducts formation in the embryonic liver of mice. The expression of Cyp1a2 (2.3-3.7 fold) suggests that the fetal skin has metabolic activation capacity and is likely to generate reactive AFB1-8,9-epoxide intermediate locally.

The similarities and differences between previous research and the current research are noted by comparing. Our results show that fetuses have a susceptible target, the skin, as well as hepatic and pulmonary tissues, which have been the major targets in studies of transplacental AFB1 toxicity **(6,7,10,11)**. The extent of molecular changes seen in skin (3.2-fold increase in expression of Trp53) is somewhat less than that seen in fetal liver (4-5-fold) **(11)**, perhaps because of differences in tissue expression of CYP450 and metabolic activation capacity. However, the uniformity of dose-response relationships and the detection of DNA adducts show that fetal skin is indeed a real target organ for genotoxicity caused by AFB1 exposure.

A few caveats must be noted. First, the analysis was limited to a single time point (E19) and further postnatal studies are required to see if the early molecular changes lead to overt neoplasia. Secondly, while the sample size (n=10 for each group) was sufficient to detect larger effect sizes, it could not have detected more subtle effects. Third, the molecular analyses were carried out on whole-skin homogenates, which precluded the determination of whether changes in gene expression were primarily in the epidermis or dermis. Fourth, the standardized gene nomenclature was used throughout the manuscript, but some antibodies used in immunohistochemical staining recognize the wild-type protein, thus restricting the interpretation of mechanisms. Postnatal longitudinal follow-up and single-cell transcriptomics will give further insight into the responses and long-term effects of prenatal AFB1 exposure that are cell-type specific.

5. Conclusion

AFB1 causes teratogenic and early pre-neoplastic changes in fetal mouse skin after gestational exposure in late pregnancy (E13-E18) such as epidermal hyperplasia, hair follicle dysplasia, activation of proliferative and apoptotic pathways and DNA adducts formation. These results are in accordance with the first step of carcinogenesis, but are not enough to prove malignant transformation. Long-term follow-up studies are needed to establish whether the early molecular changes are oncogenic in the long term. In general, these findings call for the protection of developing skin from environmental exposure to carcinogens and the need to avoid exposure to aflatoxin during pregnancy.

6. Declarations

Acknowledgments

The author gratefully acknowledges the institutional facilities and technical support that contributed to completion of this study.

Ethical Considerations

All animal procedures were approved by the Institutional Animal Care and Use Committee (Approval No: IACUC-2024-156) and conducted in accordance with ARRIVE guidelines.

Authors' Contributions

Sally Adnan Mousa AL-Rikabi conceived and designed the study, performed the experiments, analyzed the data, drafted and revised the manuscript, and approved the final version for publication.

Conflict of Interest

None declared.

Fund or Financial Support

None.

References

1. Kensler TW, Roebuck BD, Wogan GN, Groopman JD. Aflatoxin: a 50-year odyssey of mechanistic and translational toxicology. Toxicol Sci. 2011;120(Suppl 1):S28-48. [doi:10.1093/toxsci/kfq283]
2. Marchese S, Polo A, Ariano A, Velotto S, Costantini S, Severino L. Aflatoxin B1 and M1: biological properties and their involvement in cancer development. Toxins (Basel). 2018;10(6):214. [doi:10.3390/toxins10060214]
3. Smela ME, Currier SS, Bailey EA, Essigmann JM. The chemistry and biology of aflatoxin B(1): from mutational spectrometry to carcinogenesis. Carcinogenesis. 2001;22(4):535-45. [doi:10.1093/carcin/22.4.535]

4. Weng MW, Lee HW, Choi B, Wang HT, Hu Y, Mehta M, et al. AFB1 hepatocarcinogenesis is via lipid peroxidation that inhibits DNA repair, sensitizes mutation susceptibility and induces aldehyde-DNA adducts at p53 mutational hotspot codon 249. Oncotarget. 2017;8(11):18213-26. [doi:10.18632/oncotarget.15313]
5. Partanen HA, El-Nezami HS, Leppänen JM, Myllynen PK, Woodhouse HJ, Vähäkangas KH. Aflatoxin B1 transfer and metabolism in human placenta. Toxicol Sci. 2010;113(1):216-25. [doi:10.1093/toxsci/kfp257]
6. Hsieh LL, Hsieh TT. Detection of aflatoxin B1-DNA adducts in human placenta and cord blood. Cancer Res. 1993;53(6):1278-80. [PMID:8383006]
7. Smith LE, Prendergast AJ, Turner PC, Humphrey JH, Stoltzfus RJ. Aflatoxin exposure during pregnancy, maternal anemia, and adverse birth outcomes. Am J Trop Med Hyg. 2017;96(4):770-6. [doi:10.4269/ajtmh.16-0730]
8. Shuaib FMB, Jolly PE, Ehiri JE, Yatich N, Jiang Y, Funkhouser E, et al. Association between birth outcomes and aflatoxin B1 biomarker blood levels in pregnant women in Kumasi, Ghana. Trop Med Int Health. 2010;15(2):160-7. [doi:10.1111/j.1365-3156.2009.02435.x]
9. Turner PC, Collinson AC, Cheung YB, Gong Y, Hall AJ, Prentice AM, et al. Aflatoxin exposure in utero causes growth faltering in Gambian infants. Int J Epidemiol. 2007;36(5):1119-25. [doi:10.1093/ije/dym122]
10. da Silva JVB, de Oliveira CAF, Ramalho LNZ. Effects of prenatal exposure to aflatoxin B1: a review. Molecules. 2021;26(23):7264. [doi:10.3390/molecules26237264]
11. Chawanthayatham S, Thiantanawat A, Egner PA, Groopman JD, Wogan GN, Croy RG, et al. Prenatal exposure of mice to the human liver carcinogen aflatoxin B1 reveals a critical window of susceptibility to genetic change. Int J Cancer. 2015;136(6):1254-62. [PMID:25070670]
12. Hussein Khalaf R, Hosseini Khah Z. The effect of resveratrol on cervical cancer cell growth by inhibiting TGF-β gene expression. J Obstet Gynecol Cancer Res. 2026;11(1):10-6. [doi:10.24200/jogcr.11.1.10]
13. Fuchs E. Scratching the surface of skin development. Nature. 2007;445(7130):834-42. [doi:10.1038/nature05659]
14. Sennett R, Rendl M. Mesenchymal-epithelial interactions during hair follicle morphogenesis and cycling. Semin Cell Dev Biol. 2012;23(8):917-27. [doi:10.1016/j.semcdb.2012.08.011]
15. Schmidt-Ullrich R, Paus R. Molecular principles of hair follicle induction and morphogenesis. Bioessays. 2005;27(3):247-61. [doi:10.1002/bies.20184]
16. Wang Y, Tan W, Wang CC, Leung LK. Exposure to aflatoxin B1 in late gestation alters protein kinase C and apoptotic protein expression in murine placenta. Reprod Toxicol. 2016;61:68-74. [doi:10.1016/j.reprotox.2016.03.001]
17. Percie du Sert N, Hurst V, Ahluwalia A, Alam S, Avey MT, Baker M, et al. The ARRIVE guidelines 2.0: updated guidelines for reporting animal research. PLoS Biol. 2020;18(7):e3000410. [doi:10.1371/journal.pbio.3000410]
18. National Research Council. Guide for the care and use of laboratory animals. 8th ed. Washington (DC): National Academies Press; 2011. [doi:10.17226/12910]
19. Wangikar PB, Dwivedi P, Sinha N, Sharma AK, Telang AG. Effects of aflatoxin B1 on embryo fetal development in rabbits. Food Chem Toxicol. 2005;43(4):607-15. [doi:10.1016/j.fct.2005.01.004]
20. Murnyák B, Hortobágyi T. Immunohistochemical correlates of TP53 somatic mutations in cancer. Oncotarget. 2016;7(40):64910-20. [doi:10.18632/oncotarget.11912]

How to Cite This Article:

Adnan Mousa AL-Rikabi S. Aflatoxin B1-Induced Teratogenic and Early Carcinogenic Alterations in Fetal Skin and Hair Follicles of Late-Gestation Mice. J Obstet Gynecol Cancer Res. 2026;11(12):1211-1223.

Download citation: RIS | EndNote | Mendeley | BibTeX |